



# Quality assessment of ground-based microwave measurements of chlorine monoxide, ozone, and nitrogen dioxide from the NDSC radiometer at the Plateau de Bure

P. Ricaud, P. Baron, J. de La Noë

## ► To cite this version:

P. Ricaud, P. Baron, J. de La Noë. Quality assessment of ground-based microwave measurements of chlorine monoxide, ozone, and nitrogen dioxide from the NDSC radiometer at the Plateau de Bure. *Annales Geophysicae*, 2004, 22 (6), pp.1903-1915. 10.5194/angeo-22-1903-2004 . hal-00329317

**HAL Id: hal-00329317**

**<https://hal.science/hal-00329317>**

Submitted on 14 Jun 2004

**HAL** is a multi-disciplinary open access archive for the deposit and dissemination of scientific research documents, whether they are published or not. The documents may come from teaching and research institutions in France or abroad, or from public or private research centers.

L'archive ouverte pluridisciplinaire **HAL**, est destinée au dépôt et à la diffusion de documents scientifiques de niveau recherche, publiés ou non, émanant des établissements d'enseignement et de recherche français ou étrangers, des laboratoires publics ou privés.

# Quality assessment of ground-based microwave measurements of chlorine monoxide, ozone, and nitrogen dioxide from the NDSC radiometer at the Plateau de Bure

P. Ricaud<sup>1</sup>, P. Baron<sup>2</sup>, and J. de La Noë<sup>1</sup>

<sup>1</sup>Observatoire Aquitain des Sciences de l'Univers (OASU), Laboratoire d'Astrodynamique, d'Astrophysique et d'Aéronomie de Bordeaux (L3AB), CNRS/INSU, Floirac, France

<sup>2</sup>Noveltis, Toulouse, France

Received: 18 January 2002 – Revised: 21 January 2004 – Accepted: 28 January 2004 – Published: 14 June 2004

**Abstract.** A ground-based microwave radiometer dedicated to chlorine monoxide (ClO) measurements around 278 GHz has been in operation from December 1993–June 1996 at the Plateau de Bure, France (45°N, 5.9°E, 2500 m altitude). It belongs to the international Network for the Detection of Stratospheric Change. A detailed study of both measurements and retrieval schemes has been undertaken. Although dedicated to the measurements of ClO, simultaneous profiles of O<sub>3</sub>, ClO and NO<sub>2</sub>, together with information about the instrumental baseline, have been retrieved using the optimal estimation method. The vertical profiles have been compared with other ground-based microwave data, satellite-borne data and model results. Data quality shows: 1) the weak sensitivity of the instrument that obliges to make time averages over several hours; 2) the site location where measurements of good opacities are possible for only a few days per year; 3) the baseline undulation affecting all the spectra, an issue common to all the microwave instruments; 4) the slow drift of some components affecting frequencies by 3–4 MHz within a couple of months. Nevertheless, when temporally averaging data over a few days, ClO temporal variations (diurnal and over several weeks in winter 1995) from 35–50 km are consistent with model results and satellite data, particularly at the peak altitude around 40 km, although temporal coincidences are infrequent in winter 1995. In addition to ClO, it is possible to obtain O<sub>3</sub> information from 30–60 km whilst the instrument is not optimized at all for this molecule. Retrievals of O<sub>3</sub> are reasonable when compared with model and another ground-based data set, although the lowermost layers are affected by the contamination of baseline remnants. Monthly-averaged diurnal variations of NO<sub>2</sub> are detected at 40 km and appear in agreement with photochemical model results and satellite zonally-averaged data, although the amplitude is weaker than the other data sets. This NO<sub>2</sub> result highlights the great potential of the retrieval scheme used.

**Key words.** Atmospheric composition and chemistry (middle atmosphere – composition and chemistry). Meteorology and atmospheric dynamics (instruments and techniques). Radio Science (remote sensing)

## 1 Introduction

It is now well established that ozone (O<sub>3</sub>) reduction at high latitudes in winter is correlated with the activation of halogen compounds and consequently correlated with the presence of chlorine monoxide (ClO) (World Meteorological Organization (WMO), 1995). Nevertheless, at mid-latitudes, the negative trend in O<sub>3</sub> of a few percent per decade in the mid-to-upper stratosphere is still under study. Causes might be the presence of air masses of polar origin (O<sub>3</sub>-poor or ClO-rich air masses) or tropical origin with air processed through sulfate aerosols, enabling a slow activation of chlorine species. So far, the most extensive study involving ClO has been performed with measurements from the Microwave Limb Sounder (MLS) instrument aboard the Upper Atmosphere Research Satellite (UARS) from 1991 to 1997 (Waters et al., 1996). An averaged positive ClO trend of about 0.1 ppbv per decade has been observed at 2.1 hPa from 70°S to 70°N (Froidevaux et al., 2000). Studies of northern mid-latitudes processes were conducted by, for example, Santee et al. (2000) and Klein et al. (2000). Ricaud et al. (2000) and Raffalski et al. (1998) have concentrated in their publications on the diurnal cycle and the seasonal variations of ClO in the Northern Hemisphere.

In terms of ground-based instruments, little information is available at mid-latitudes essentially because only microwave techniques can detect weak ClO lines for periods when halogens are not activated. Indeed, the great majority of the ground-based microwave instruments dedicated to ClO observations and belonging to the Network for the Detection of Stratospheric Change (NDSC) are located at high latitudes for arctic studies (e.g. Raffalski et al., 1998; Ruhnke

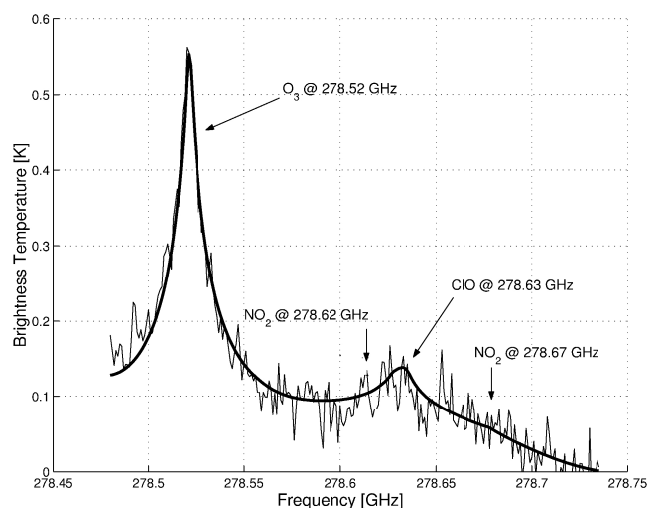


**Fig. 1.** Stratospheric brightness temperature from the zenith direction for a measured spectrum averaged over 1995 (thick line) and a 15-min. integration spectrum measured on 5 January 1995 (thin line). Contributions from O<sub>3</sub>, ClO and NO<sub>2</sub> are quoted. Only the 1-MHz channels are shown. Baseline ripples are not subtracted from the measurements.

et al., 1999; Klein et al., 2000) and antarctic studies (e.g. de Zafra et al., 1989; Solomon et al., 2002). At mid-latitudes, a ClO microwave radiometer operating around the frequency of 278 GHz enabling the detection of O<sub>3</sub>, ClO and NO<sub>2</sub> lines, and already described in detail in Ricaud et al. (1997), has been installed at the Plateau de Bure (44.6°N, 5.9°E, 2500 m) in the French Alps. Spectra have been measured from December 1993 to June 1996 during times of low opacities before the instrument was sent to Mauna Kea, in order to perform a comparison with another instrument already installed at that site (Ricaud et al., 1998). We can note that another ClO microwave instrument developed under European contracts, the European Minor Constituent Radiometer (EMCOR), operating around 205 GHz and using SIS technology mixer (Maier et al., 2001), is installed in the northern mid-latitudes in the Swiss Alps, at the Jungfraujoch summit (3580 m altitude).

A first analysis has been reported, using the Optimal Estimation Method (Rodgers, 1990) to estimate ClO vertical profiles on a limited segment of the Plateau de Bure data, using the technique of “day – night” differencing to reduce baseline ripples (Ricaud et al., 1997). As the O<sub>3</sub> signal and the first-order baseline artifacts are removed by this procedure, only ClO profiles have been retrieved between 25 and 55 km. In order to optimize the amount of information contained in the spectra, i.e. in order to bring O<sub>3</sub> and NO<sub>2</sub> profiles together with ClO profiles, a method proposed by Kuntz et al., (1997) which does not require “day – night” differencing has now been implemented. The same philosophy is now used when analyzing measurements provided by the Sub-Millimetre Radiometer (SMR) instrument aboard the Odin satellite (Baron et al., 2002) with the forward model and re-

trieval code Microwave Odin Line Estimation and Retrieval (MOLIERE). This code has been modified to take into account an uplooking geometry, and its latest version is used to retrieve O<sub>3</sub> information from the microwave instrument operating at 110 GHz in Bordeaux (Schneider et al., 2003).

Spectra measured at the Plateau de Bure are analysed by retrieving simultaneously ClO, O<sub>3</sub>, and NO<sub>2</sub> profiles, together with baseline parameters. The aim of this paper is to present the new retrieval scheme, and to assess the quality of the measurements by comparing with profiles measured by ground-based or satellite-borne instruments and model results. In Sect. 2, the observational technique is described and the baseline is characterized. In Sect. 3, the retrieval scheme is defined and retrieval from synthetic spectra are simulated in order to estimate the capabilities of the present instrument. In Sect. 4, we present the first results of the analysis over the period from January to April 1995, and the comparisons with ground-based and satellite-borne instruments and models for ClO, O<sub>3</sub>, and NO<sub>2</sub>.

Ozone measurements are compared with measurements obtained by another ground-based microwave radiometer operating at the same latitude and situated at Bern University (46.9°N, 7.4°E), measuring the ozone line at 142 GHz (Peter and Kämpfer, 1995). Output of the purely photochemical zero-dimensional (0-D) model (Ricaud et al., 1994) and the SLIMCAT three-dimensional (3-D) chemical transport model (Chipperfield, 1999) are also compared with the O<sub>3</sub> measurements. The retrieved ClO profiles are compared with these two models, and, whenever available, with the ClO measurements version 4 from the UARS/MLS instrument (Barath et al., 1993). The measured NO<sub>2</sub> diurnal variations are compared with the purely photochemical model and with the Version 8 zonally-averaged measurements from the Cryogenic Limb Array Etalon (CLAES) instrument aboard the UARS satellite (Roche et al., 1993).

## 2 Measurement description

### 2.1 Stratospheric brightness temperature from the zenith direction

For a detailed description of the instrument and its measurement principle, the reader should refer to Ricaud et al. (1997). A general description is nevertheless presented below. The millimeter-wave instrument is a heterodyne receiver with three filter banks covering a bandwidth of 506 MHz: 30 channels of 5 MHz on the left side of the bandwidth, 256 channels of 1 MHz at the center, and 20 channels of 5 MHz on the right side. The O<sub>3</sub> line (278.520 GHz) and the ClO hyperfine lines (278.631 GHz) are both covered by the 1-MHz channels. The bank of 1-MHz channels also contains weak NO<sub>2</sub> lines, the two strongest being at 278.621 and 278.677 GHz (Fig. 1).

The observing method is the beam switching technique (Parrish et al., 1988) where atmospheric emission is measured both at high elevation, named “reference” (R), and at

low elevation, named “signal” (S). A dielectric sheet of appropriate emissivity is mounted at Brewster’s angle within the (R) beam, acting as a gray-body emitter to equalize the continuum power levels in the (S) and (R) beams. The (S) beam elevation is then continuously and automatically adjusted to keep the continuum levels equal as the tropospheric opacity changes.

Integration time is 15 minutes. Data are stored as (S-R)/R spectra which are proportional to the stratospheric emission from the zenith direction (Lezeaux, 1999). The factor of conversion from [(S-R)/R] to stratospheric brightness temperature from the zenith direction  $y$  is:

$$y = \frac{[R]}{[A_{st}^s e^{-A_t^s \tau_z} - A_{st}^r e^{-A_t^r \tau_z} e^{-\tau_d}]} [(S-R)/R], \quad (1)$$

where  $A_{st}^s$  and  $A_{st}^r$  represent the stratospheric air masses in the (S) and (R) beam, respectively;  $A_t^s$  and  $A_t^r$  represent the tropospheric air masses in the (S) and (R) beam, respectively;  $\tau_z$  is the tropospheric opacity;  $\tau_d$  is the dielectric sheet opacity. The term  $[R]$  is the system temperature in the [R] beam and can be expressed as:

$$[R] = T_{\text{rec}} + T_{\text{atm}}(1 - e^{-A_t^r \tau_z})e^{-\tau_d} + T_d(1 - e^{-\tau_d}), \quad (2)$$

where  $T_{\text{rec}}$  is the receiver noise temperature,  $T_{\text{atm}}$  is the physical mean temperature of the troposphere,  $T_d$  is the physical temperature of the dielectric sheet. The term  $T_{\text{atm}}(1 - e^{-A_t^r \tau_z})$  corresponds to the tropospheric emission deduced from a simple model of an isothermal troposphere. Mean tropospheric temperature is estimated by subtracting 6 K from the surface temperature. In order to determine the receiver temperature, a calibration process is automatically performed every 8 spectra. Twice per month, a manual calibration was also carried out. Receiver temperature determined by the automatic procedure exhibits a strong sine wave ripple. Such a ripple does not appear on manually calibrated procedures but its mean value shows large fluctuations over a period of several months. Knowing that, we decided to use the manual calibration to determine the  $T_{\text{rec}}$  vector, whose mean value is corrected to be equal to the mean value of  $T_{\text{rec}}$  given by the automatic procedure. We can rewrite Eq. (1) as:

$$y = \frac{[(S-R)]}{\eta}, \quad (3)$$

where  $[(S-R)]$  is the difference between (S) and (R) and  $\eta = A_{st}^s e^{-A_t^s \tau_z} - A_{st}^r e^{-A_t^r \tau_z} e^{-\tau_d}$ . Radiometric noise on the  $[(S-R)]$  is given for a single side band receiver as:

$$\sigma = \frac{2T_{\text{sys}}}{\sqrt{\delta\nu \delta t}}, \quad (4)$$

where  $T_{\text{sys}}$  is the system noise temperature,  $\delta\nu$  is the frequency width of a given channel, and  $\delta t$  is the integration time for measuring a single spectrum, i.e. 15 minutes. From Eq. (3), the radiometric noise on the stratospheric brightness temperature from the zenith direction is deduced to be  $\sigma/\eta$ .

As shown in Fig. 2, variations of the value of the  $1/\eta$  parameter are mainly induced by the atmospheric opacity. The

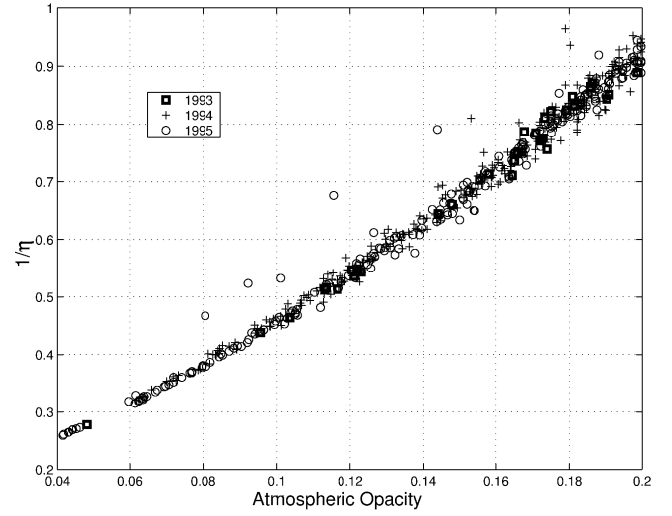


**Fig. 2.** Variation of the factor  $(1/\eta)$  with the atmospheric opacity for the 1-MHz channels.

highest opacity for which measurements are taken into account in this study is  $\tau_z=0.2$ , giving a value of  $1/\eta$  close to 1. The associated thermal (i.e. random) noise amplitude in the stratospheric signal is 0.067 K per channel, giving a signal-to-noise ratio (SNR) close to 1, considering a midday CIO signal and a 15-minute integration period. When considering a nighttime  $\text{NO}_2$  signal at 278.677 GHz (the strongest line), the SNR is close to 0.3. The lowest measured atmospheric opacity is about  $\tau_z=0.04$  which gives a much smaller thermal noise of about 0.017 K ( $1/\eta=0.25$ ) per channel, giving a SNR of  $\sim 4$ , considering a midday CIO line. When considering a nighttime  $\text{NO}_2$  line at 278.677 GHz, the associated SNR is close to 1.

The Schottky mixer technology of the 1980s employed for the Bure instrument gives a receiver noise temperature of  $\sim 850$  K. State-of-the-art microwave instruments using a SIS technology mixer can reach receiver noise temperature close to 100 K (see e.g. Maier et al., 2001), i.e. the integration time can be reduced by a factor of  $\sim 60$ . The poor Bure instrument sensitivity implies the need to integrate over several hours.

Another limitation in the analysis of the Bure measurements is the small number of periods of good quality (typically  $\tau_z < 0.08$ ) during both daytime and nighttime at the site of the Plateau de Bure. From December 1993 to April 1995 (refer to Ricaud et al., 1997), the best period was the time frame from January to April 1995. We will then focus on this particular period for assessing the quality of the measurements of  $\text{O}_3$ , CIO, and  $\text{NO}_2$ .

## 2.2 Baseline characterisation

The shape of the instrumental baseline (Ricaud et al., 1997) has been measured in February 1994 and in January 1995 (Figs. 3 and 4, respectively). A simple function over the total bandwidth cannot fit the baseline undulation. A first analysis representing the baseline as a tenth-order polynomial whose

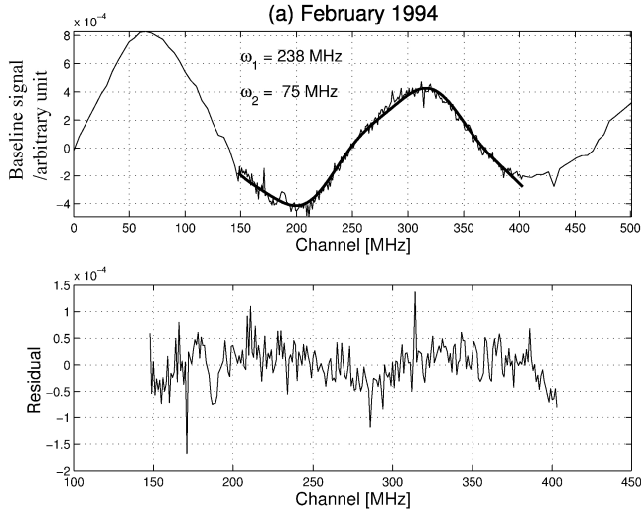


**Fig. 3.** Upper: Baseline (arbitrary unit) measured in February 1994 (thin line) and fit of the signal over the 1-MHz channels with sine functions (thick line). Lower: Residual between the fit and the measured baseline over the 1-MHz channels. Note that the retrieved amplitude of the baseline ripples is typically ranging from 5 to 20 mK.

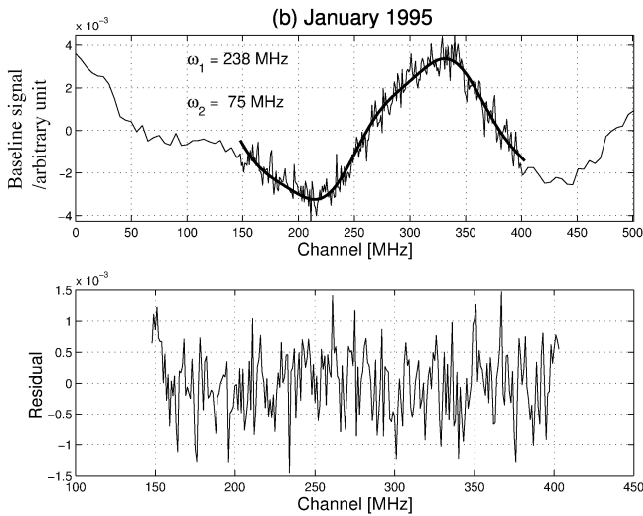


**Fig. 4.** Same as Figure 3 but for a baseline measured in January 1995.

the amplitude was retrieved simultaneously with the vertical profiles gave too much ClO below 35 km. Since baseline ripples which are caused by reflections in the system optics usually appear sinusoidally, we have decided to limit our present analysis to the central 256 channel high-resolution section of the spectrometer, where the baseline ripple more closely resembles a simple sine wave function with a period of  $\sim 230$  MHz. In the earlier analysis by Ricaud et al. (1997), a 70 MHz ripple was also mentioned with an amplitude of less than 5 mK on a spectrum from the zenith direction. Although the intensity of this ripple is 10 times smaller than the dominant ripple, studies show that even this undulation may

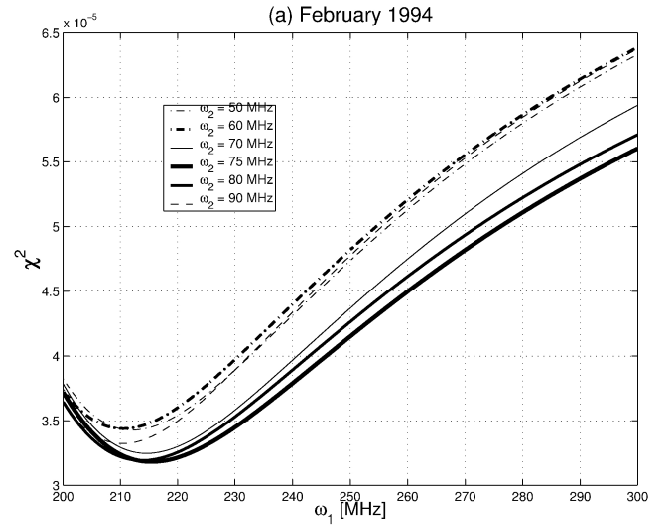


**Fig. 5.**  $\chi^2$  of the residual for different values of  $\omega_1$  and  $\omega_2$  for the baseline measured in February 1994.

induce errors on the retrieval of O<sub>3</sub> and ClO below 35 km. We must note that residuals in February 1994 (they are less marked in January 1995) show another sinusoid whose amplitude is 10 times less than the two selected sine functions. Since in Sect. 4, we will concentrate on the period January–April 1995, the baseline in the present analysis is fitted with the function  $\phi(v)$ :

$$\begin{aligned} \phi(v) = & a_1 + a_2 v + a_3 \cos\left(\frac{2\pi}{\omega_1} v\right) + a_4 \sin\left(\frac{2\pi}{\omega_1} v\right) \\ & + a_5 \cos\left(\frac{2\pi}{\omega_2} v\right) + a_6 \sin\left(\frac{2\pi}{\omega_2} v\right), \end{aligned} \quad (5)$$

where  $a_1$  and  $a_2$  represent an offset and a linear slope, respectively, and  $\omega_1$  and  $\omega_2$  are the periods of the two different sine functions. The two values giving the lowest  $\chi^2$  have been calculated to be  $\omega_1=215$  MHz and  $\omega_2=75$  MHz in February 1994, and  $\omega_1=238$  MHz and  $\omega_2=75$  MHz in January 1995 (Figs. 5 and 6, respectively). Note that the retrieved amplitude of the baseline ripples (see next section) is typically ranging from 5 to 20 km, that is consistent with the previous analysis of Ricaud et al. (1997).

### 3 Data analysis

#### 3.1 Optimal estimation method

Following the methodology developed by Kuntz et al. (1999) and used on a regular basis to analyze microwave measurements from the Odin satellite (Murtagh et al., 2002), the difference between the retrieved parameters,  $\hat{\mathbf{x}}^p$ , and the true one,  $\mathbf{x}^p$ , can be expressed as:

$$\begin{aligned} \hat{\mathbf{x}}^p - \mathbf{x}^p = & (\mathbf{A}^{p/p} - \mathbf{1})(\mathbf{x}^p - \mathbf{x}_a^p) \\ & + \sum_{q \neq p} \mathbf{A}^{p/q}(\mathbf{x}^q - \mathbf{x}_a^q) + \mathbf{D}_y \mathbf{K}_b \epsilon_b + \mathbf{D}_y \epsilon_m, \end{aligned} \quad (6)$$

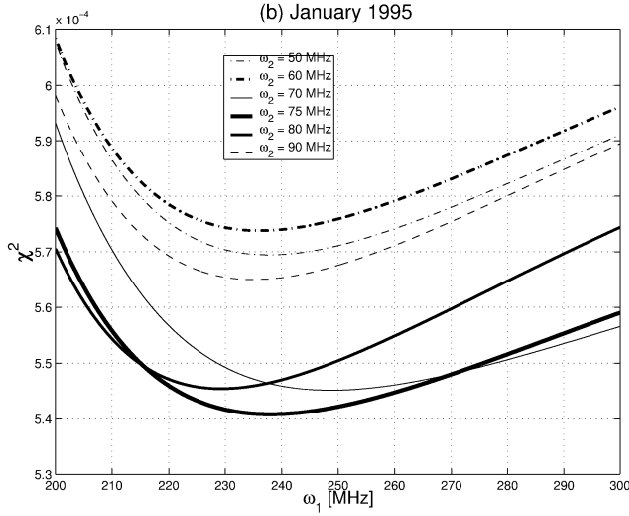


**Fig. 6.** Same as Fig. 5 but for a baseline measured in January 1995.

where  $p$  and  $q$  denote either the volume mixing ratio (VMR) profiles or baseline parameters,  $(\mathbf{A}^{p/p} - \mathbf{1})(\mathbf{x}^p - \mathbf{x}_a^p)$  is the smoothing error,  $\mathbf{A}^{p/q}(\mathbf{x}^q - \mathbf{x}_a^q)$  is the error due to the poor a-priori knowledge of other parameters to be retrieved,  $\mathbf{D}_y \mathbf{K}_b \epsilon_b$  is the error due to uncertainties in the forward model parameters, and  $\mathbf{D}_y \epsilon_m$  is the error due to the measurement uncertainties.

This expression shows that the error on the a priori value given for one parameter may induce an error on the other retrieved parameters. This effect is named contamination in Baron et al. (2002). We then may define the measurement sensitivity  $\mathbf{W}_m$  of the constituent  $\mathbf{x}^p$  as

$$\mathbf{W}_m(i) = \sum_j \mathbf{A}^{p/p}(i, j) \frac{\mathbf{x}_a^p(j)}{\mathbf{x}_a^p(i)}, \quad (7)$$

where  $i$  and  $j$  correspond to height indices. It corresponds to the weight of the measurement relative to the weight of the a priori information upon the retrieved quantity. Ideally, the measurement sensitivity for an optimal retrieval is 1. Nevertheless, we consider that the vertical domain where the retrieval is efficient to be characterized by a value of  $\mathbf{W}_m$  greater than 0.7, i.e. at least 70% of the retrieved information comes from the measurement and less than 30% from the a priori information.

The vertical resolution of the measurements is commonly defined by the width at half-maximum of the averaging kernels  $\mathbf{A}^{p/p}$ . Consequently, a high-vertical resolution data set  $\mathbf{x}_0^p$  (e.g. model results) can be degraded into a low-vertical resolution data set  $\hat{\mathbf{x}}_0^p$  by simplifying Eq. (6) into:

$$\hat{\mathbf{x}}_0^p - \mathbf{x}_0^p = (\mathbf{A}^{p/p} - \mathbf{1})(\mathbf{x}_0^p - \mathbf{x}_a^p). \quad (8)$$

Considering a 15-min integration time, the averaging kernels  $\mathbf{A}^{p/p}$  are shown in Fig. 7. The vertical resolution of the retrieved profiles and the altitude range of a good sensitivity to the measurement are deduced from the width of

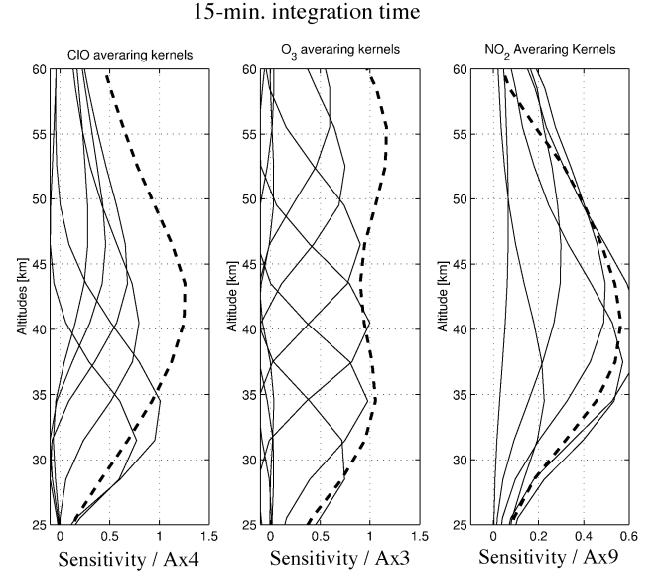


**Fig. 7.** Averaging kernels calculated from 28 to 58 km by a step of 6 km (thin line) and measurement sensitivity (thick dash line) for CIO, O<sub>3</sub> and NO<sub>2</sub>, representative of a 15-minute integration time.

the averaging kernels  $\mathbf{A}^{p/p}$  and from their sum close to 1, respectively. Thus, O<sub>3</sub> profiles are retrieved between 30–60 km with a vertical resolution of about 10–20 km and CIO profiles between 35–50 km with a vertical resolution of about 10–20 km. The measurement sensitivity for NO<sub>2</sub> has a peak at 40 km of 0.4, lower than the limit of 0.7 chosen above for  $\mathbf{W}_m$ .

A theoretical study has been performed in order to characterize the retrieval of the different parameters during either daytime or nighttime periods representative of a typical 15-minute integration time. Simulations are performed by considering an error of 1 ppbv for CIO, 8 ppmv for O<sub>3</sub>, and 10 ppbv for NO<sub>2</sub> on the a priori profile. Only thermal noise has been assumed, and its amplitude has been taken to be 0.02 K; that is consistent with a period of very low opacity, i.e. the best atmospheric conditions. Figures 8 and 9 show the retrieval studies for the daytime and the nighttime conditions, respectively. The true profile  $\mathbf{x}$ , the a priori profile  $\mathbf{x}_a$ , and the estimated profile  $\hat{\mathbf{x}}$  are represented by a solid line, by a dotted line and by stars, respectively. Shaded areas are representative of the vertical domain where an efficient retrieval is expected, i.e.  $\mathbf{W}_m > 0.7$ . Horizontal error bars are given at a one-sigma level. Daytime and nighttime O<sub>3</sub> amounts are relatively well estimated. Daytime and nighttime CIO retrievals are strongly contaminated by the a priori profile, except around 40 km. In other words, this simulation based on a 15-min. integration time shows the extreme difficulty of retrieving information on CIO outside the altitude domain centered at 40 km, where the measurement response is close to 1, even considering the best atmospheric conditions. Daytime NO<sub>2</sub> estimates are essentially a priori contaminated while nighttime estimates are more affected by information contained in the measurements.

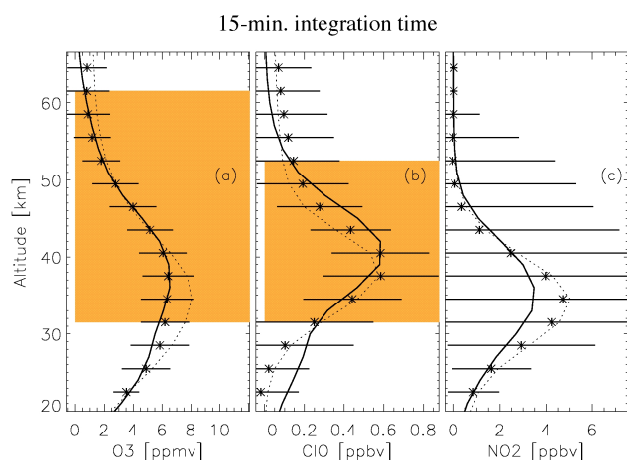


**Fig. 8.** Simultaneously estimated daytime profiles (stars) from noise-free synthetic spectrum of (a)  $\text{O}_3$ , (b)  $\text{ClO}$ , and (c)  $\text{NO}_2$ , together with: true profile (thick line) and a priori profile (dotted line), representative of a 15-minute integration time. Thermal noise error bars are given at  $1\text{-}\sigma$  level. The shaded area corresponds to a vertical domain where an efficient retrieval is expected, namely  $W_m > 0.7$ . Simultaneous retrievals from a noise-free spectrum represent the best-case scenario, thus the conclusions drawn can be considered as optimal.

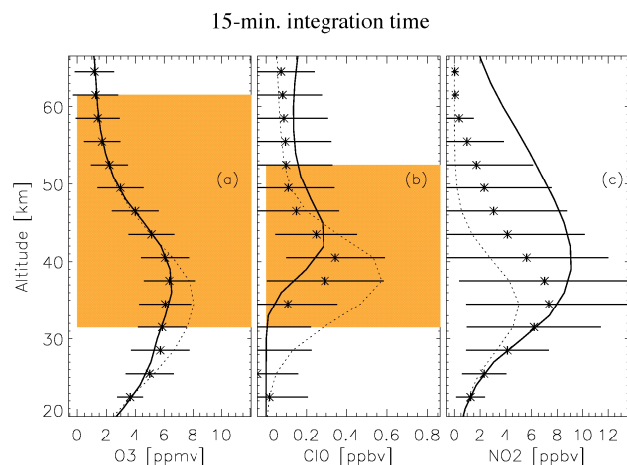


**Fig. 9.** Same as Fig. 8 but for nighttime profiles.

The study above only takes into account thermal noise that is considered as an uncorrelated source of random error. From Ricaud et al. (1997), it has been noted that essentially two other sources of error will need to be considered: spectroscopic and baseline errors. These terms might be treated as systematic errors (see, e.g. de La Noë et al., 1998). Baseline error dominates retrievals in the lower part of the stratosphere and spectroscopic error in the upper part, although the random error induced by the thermal noise always dominates. Since the number of averaged vertical profiles differs from one day to another, we have chosen to present for each Bure data only the random error associated. The systematic error can be estimated to be in the worst case 80% of

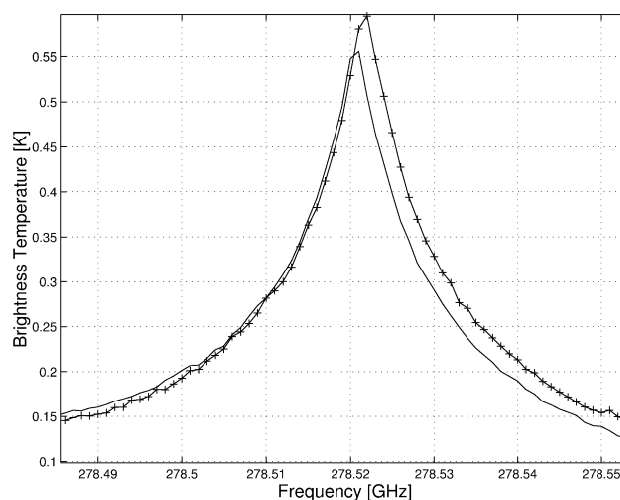


**Fig. 10.** Ozone line measured in January 1995 (solid line) and in March 1995 (crosses).

the random error on a 15-min. integration time (Ricaud et al., 1997), namely 0.5 ppmv for  $\text{O}_3$  VMR, 0.15 ppbv for  $\text{ClO}$  VMR, and 4 ppbv for  $\text{NO}_2$  VMR. These systematic errors are represented on each figure.

In addition to this study, comparison of a set of average spectra measured at different periods during winter 1995 shows a frequency shift of the instrument (Fig. 10). The frequency seems to drift continuously with time. In order to take into account this effect the frequency shift is retrieved simultaneously with the other parameters. Such a retrieval is nonlinear and is solved by using an iterative scheme. For a given retrieval, the first guess of the frequency is the frequency retrieved from the previous measurement. The iterative process converges after 2–3 iterations. Figure 11 shows the evolution of the retrieved frequency shift within the period 1993–1996 with respect to the value estimated in January 1994. A maximum deviation of 3.5–4 MHz has been estimated.

## 4 Quality assessment of $\text{O}_3$ , $\text{ClO}$ and $\text{NO}_2$ measurements

### 4.1 Winter variations

In order to assess the quality of the measurements performed by the radiometer installed at the Plateau de Bure, we have used three different sets of data: ground-based and satellite measurements, together with model results. Independent comparison measurements of  $\text{O}_3$  come from the ground-based microwave radiometer installed at the University of Bern, Switzerland. Comparison measurements of  $\text{ClO}$  are taken from the UARS/MLS instrument and comparison measurements of  $\text{NO}_2$  are from the UARS/CLAES instrument. The theoretical results of  $\text{O}_3$ ,  $\text{ClO}$  and  $\text{NO}_2$  are deduced from a purely photochemical zero-dimensional (0D) model and from the three-dimensional (3D) chemical transport model

SLIMCAT. Following the analysis described in (Ricaud et al., 2000), the 0D-model was run according to two scenarios. The yield in the reaction  $\text{ClO} + \text{OH} \rightarrow \text{HCl} + \text{O}_2$  is either 5% (case A) or 10% (case B), and is an important issue in the understanding of the temporal evolution of the chlorine budget (see, e.g. Lary et al., 1995). The vertical resolution of the models and of the satellite data have been degraded to match the resolution of the Bure measurements by using Eq. (8). Since the vertical resolution of the ground-based microwave measurements of  $\text{O}_3$  from Bern is similar to the one from Bure, no degradation have been performed upon the Bern data.

Although the Bure instrument is dedicated to  $\text{ClO}$  measurements, the  $\text{O}_3$  line is much stronger than  $\text{ClO}$  lines. Consequently,  $\text{O}_3$  retrievals are expected to be more reliable than  $\text{ClO}$  retrievals; thus, we start with the  $\text{O}_3$  results. Retrievals of  $\text{O}_3$  from Bure (see Fig. 12) centered at 31.5 km appear to be scattered around both the Bern measurements and the SLIMCAT model results, tracing the incidence of a remnant of baseline structure that can affect the retrievals in the lower part of the stratosphere. Higher up, Bure retrievals are consistent with SLIMCAT model outputs, although the amount of  $\text{O}_3$  from Bern is less or equal to the amount of  $\text{O}_3$  from Bure. The best agreement between the three data sets appears to be in the layers 43.5 and 49.5 km. In addition, the  $\text{O}_3$  pronounced minimum at the end of January 1995 at 37.5 km is well detected in Bure, in agreement with SLIMCAT and Bern data.

The temporal evolution of  $\text{ClO}$  over the same period as measured at Bure and as calculated by the 3D model is shown in Fig. 13, together with some measurements from the UARS/MLS instrument. The MLS instrument samples an area of the atmosphere from  $34^\circ$  on one side of the equator to  $80^\circ$  on the other side, the hemisphere of high-latitude coverage alternating every  $\sim 35$  days. It appears that for this particular winter period only 6 days of measurements are available: 1 and 3 February 1995, and 6, 7, 8 and 10 March 1995. For these six days, UARS/MLS data have been zonally-averaged from  $40^\circ\text{N}$  to  $50^\circ\text{N}$ , in order to reduce measurement errors, and daytime data measured between 11:00 and 15:00 Local Solar Time (LST) have been selected. Note the difference between SLIMCAT model high vertical resolution output (thin crosses) and low vertical resolution output (thick crosses). Except at the altitude of the maximum, namely 37.5 km, the altitude resolution can alter the  $\text{ClO}$  VMR by  $\sim 0.25$  ppbv and  $\sim 0.15$  ppbv at 43.5 and 49.5 km, respectively.

At 31.5 km, Bure  $\text{ClO}$  VMR is consistent with UARS/MLS and is much less than SLIMCAT, although this layer has a weak instrument sensitivity of 0.5. The minimum in the  $\text{O}_3$  field observed and calculated at the end of January 1995 at 31.5 km is correlated with a maximum in both the modelled and the measured  $\text{ClO}$  at the same altitude, showing a difference of  $\sim 0.2$  ppbv between 20 and 30 January. This episode can be associated with some high values of potential vorticities (not shown), i.e. with the crossing of the Arctic vortex over southern France. This effect does not appear in the UARS/MLS data, since they have been zonally-

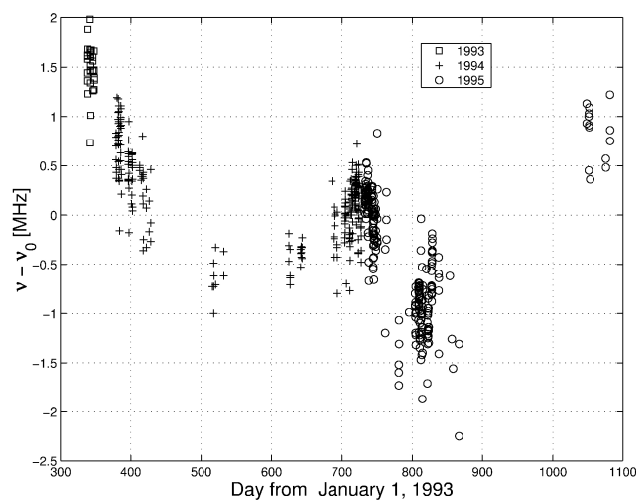


**Fig. 11.** Temporal evolution of the difference between the retrieved frequency ( $\nu$ ) and the frequency ( $\nu_0$ ) as defined at the beginning of January 1994.

averaged in order to lessen error bars. At 37.5 km,  $\text{ClO}$  VMR from Bure shows a net increase from the beginning of January to end of January in agreement with SLIMCAT, although VMR from Bure is less than SLIMCAT but very consistent with UARS/MLS  $\text{ClO}$  for the period 1 and 3 February 1995. At 43.5 km, UARS/MLS and SLIMCAT agree well, together with Bure data in January 1995. In March, data from Bure appear to be more scattered around SLIMCAT, although the March to April decrease in  $\text{ClO}$  VMR is seen both in SLIMCAT and in Bure data. At 49.5 km, UARS/MLS data is systematically less than SLIMCAT whilst Bure data is consistent with SLIMCAT. The scattering of Bure data in March–April although not negligible, is within the systematic errors of  $\sim 0.2$  ppbv. Higher up at 55.5 km, UARS/MLS measurements are much weaker than both SLIMCAT and Bure. Again, in January, Bure data appear to be very stable and in March–April more scattered. But in this layer, the instrument sensitivity is weak:  $\sim 0.5$ .

#### 4.2 Diurnal variations

Another way to assess the quality of the measurements is to concentrate on the diurnal variations of the constituents, since  $\text{O}_3$  diurnal variations (see, e.g. Zommerfelds et al., 1989),  $\text{ClO}$  diurnal variations (see, e.g. Solomon et al., 1984) and, to a lesser extent,  $\text{NO}_2$  diurnal variations have been intensively studied. We globally average data irrespectively of the year for the month of January in 12 bins of a 2-hour width, in order to study the diurnal variations of the constituents. We then compare the measured diurnal variations of  $\text{O}_3$  between 50 and 60 km with the ones calculated by the 0-D model (see Fig. 14), keeping in mind that the a priori information does not diurnally evolve (flat line). Differences in absolute values between measured and modelled variations ( $< 1$  ppmv) are mainly attributed to differences in the amount of  $\text{H}_2\text{O}$  that strongly controls  $\text{O}_3$  in the upper stratosphere



## O<sub>3</sub>-VMR starting 1 January 1995

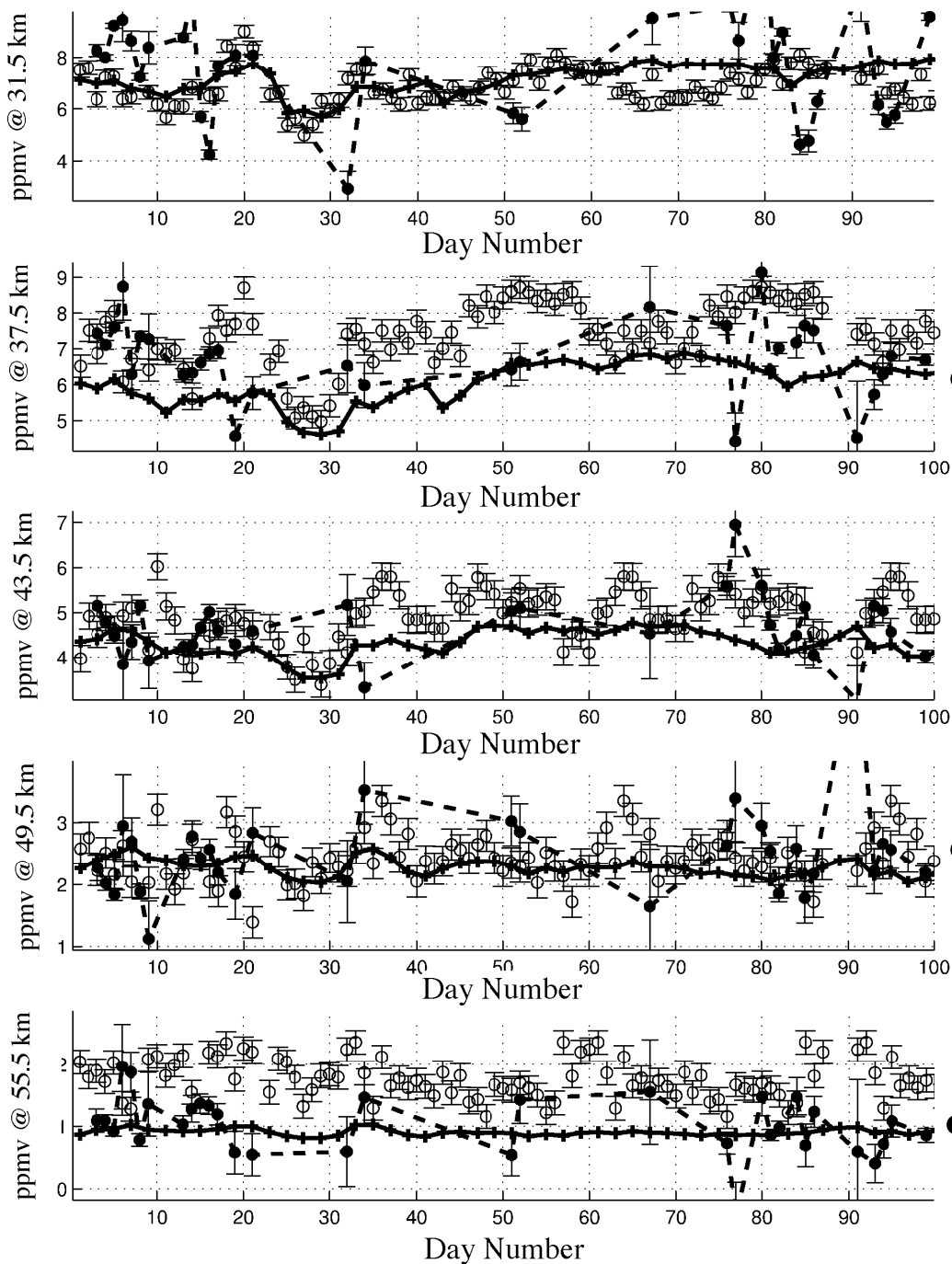


**Fig. 12.** Variations of O<sub>3</sub> VMR from January to April 1995 at 31.5, 37.5, 43.5, 49.5 and 55.5 km (from top to bottom), as retrieved from measurements by the radiometer installed at the Plateau de Bure (filled circles connected by dashed line) and by the radiometer installed at Bern (Switzerland) (open circles) and as calculated by the 3-D CTM SLIMCAT model (crosses connected by solid line) within the same layers. Note that vertical resolution of the model has been degraded to match the resolution of the ground-based measurements. Only an uncorrelated 1- $\sigma$  error due to the thermal noise is considered in the errorbar. A systematic 1- $\sigma$  error for the Bure measurements (filled circle and thick line) is represented on the right-hand side of each box.

## CIO-VMR starting 1 January 1995

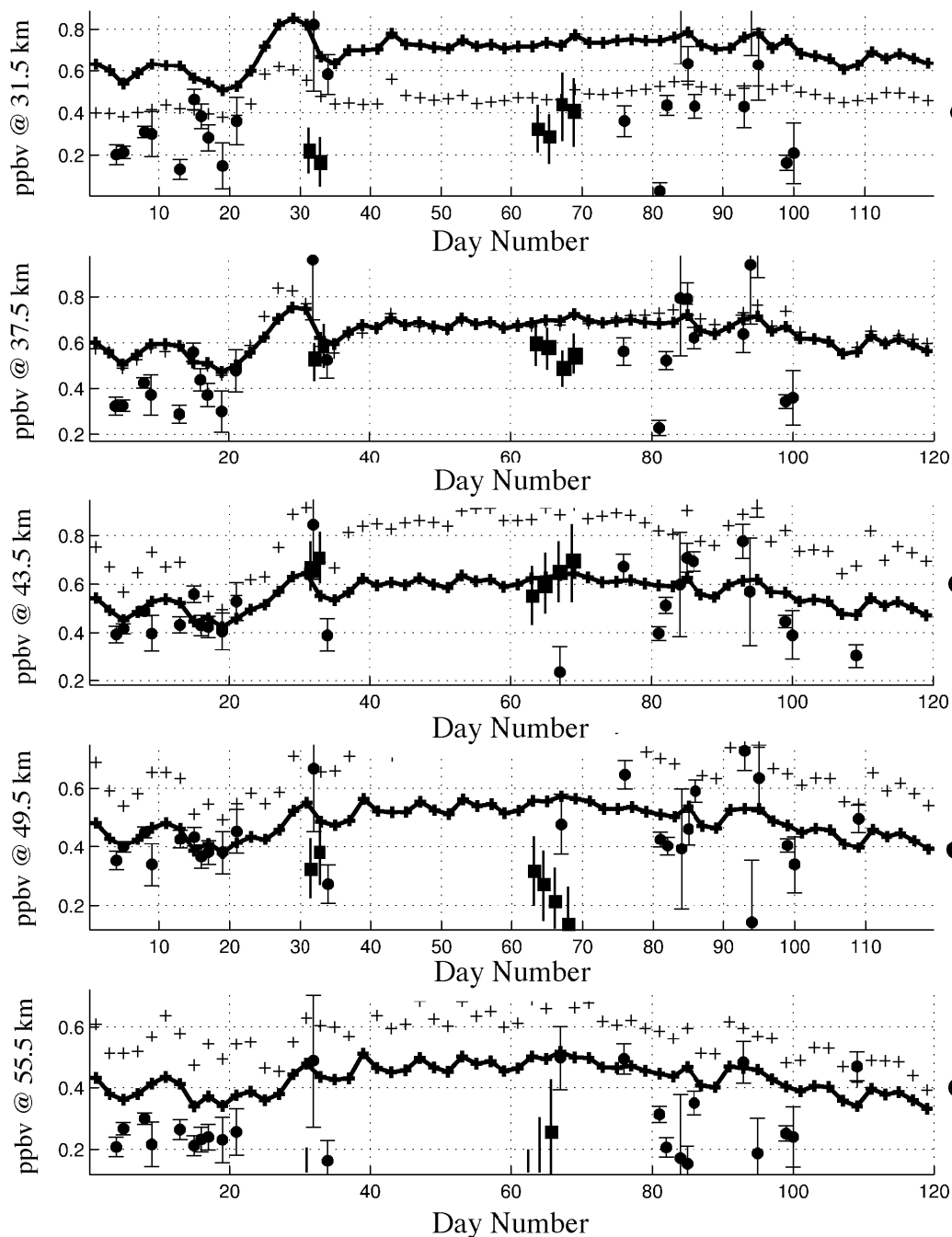


**Fig. 13.** Variations of daytime CIO VMR from January to April 1995 at 31.5, 37.5, 43.5, 49.5 and 55.5 km (from top to bottom), as retrieved from measurements by the radiometer installed at the Plateau de Bure (filled circles), as measured by the UARS/MLS instrument (squares), and as calculated by the 3-D CTM SLIMCAT model (thick crosses) within the same layers. Note that vertical resolution of the model and of the satellite data has been degraded to match the resolution of the ground-based measurements. For information, high resolution outputs from the 3-D model are also plotted (thin crosses). Only an uncorrelated 1- $\sigma$  error due to the thermal noise is considered in the errorbar. Satellite data have been zonally-averaged within the latitude band 40°N–50°N, and only data measured between 11:00 LST and 15:00 LST have been considered as daytime measurements. A systematic 1- $\sigma$  error for the Bure measurements (filled circle and thick line) is represented on the right-hand side of each box.

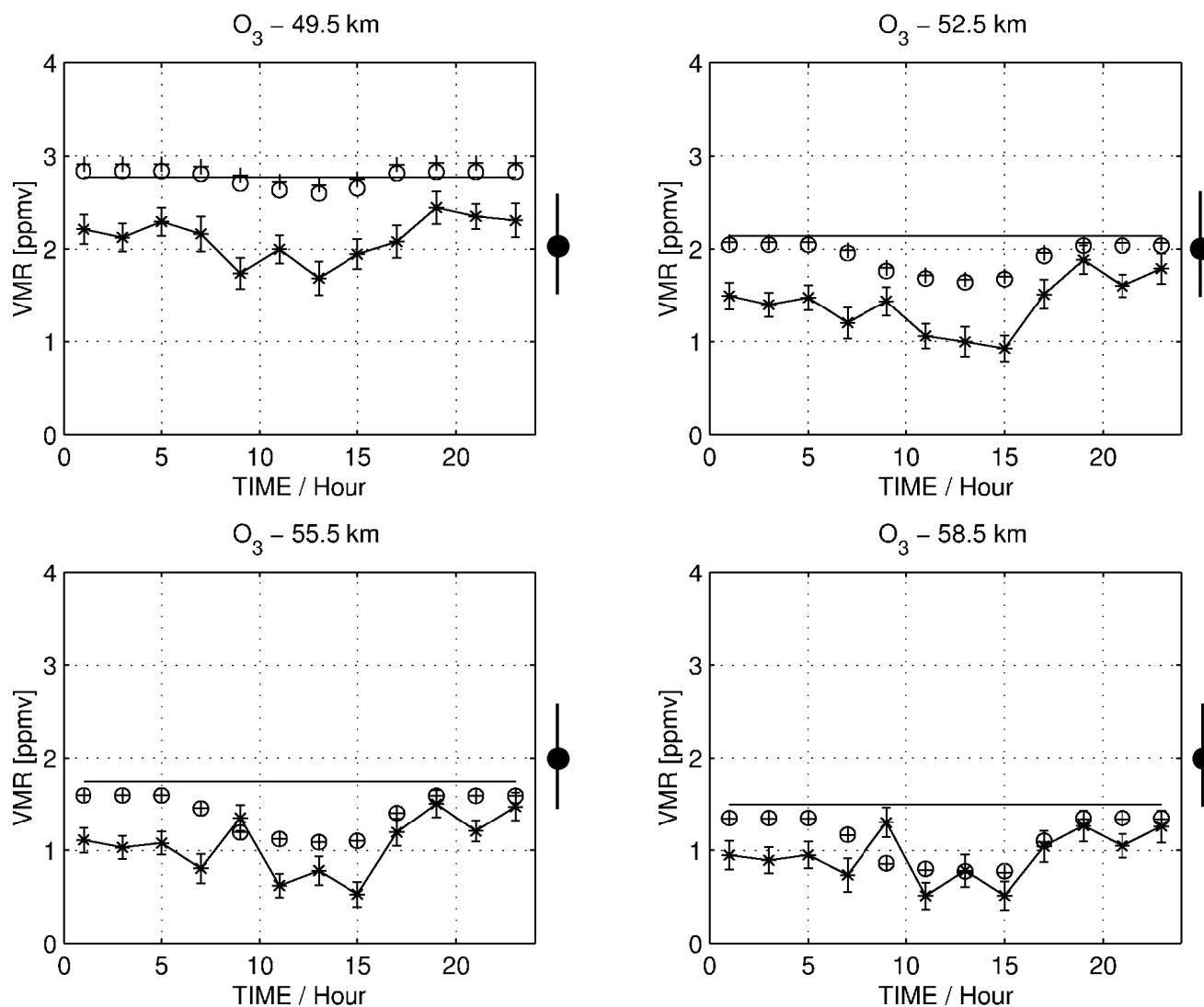


**Fig. 14.** Measured diurnal variations of O<sub>3</sub> (stars) at 49.5, 52.5, 55.5 and 58.5 km, together with the a priori value (solid line), and calculations from the 0-D model: run A (crosses) and run B (open circles). Only an uncorrelated 1-σ error due to the thermal noise is considered in the errorbar. Systematic 1-σ error for the Bure measurements (filled circle and thick line) is represented on the right-hand side of each box.

and lower mesosphere (see, e.g. Ricaud et al., 1996). The amplitude of the variations is in very good agreement between measurements and models, which gives some confidence in the instrument calibration procedures and the general deconvolution process being used.

Diurnal variations of ClO measured and modelled from 30 to 55 km are presented in Fig. 15. The amplitude of the ClO diurnal variations at 28.5 km is measured to be less than that calculated by 0.25 ppbv, but this layer has a weak instrument sensitivity of 0.5, thus the a priori contamination is far from being negligible. At 34.5 km, the difference between measurements and the model reduces to 0.1 ppbv to reach 0.05 ppbv to the daylight hours at 40.5 km, a layer where the instrument sensitivity is optimum. Above, at 46.5 km, the weak diurnal amplitude is well measured and modelled, but the ClO VMR from Bure has a deficit of ~0.2 ppbv com-

pared to the 0-D model. It is difficult enough to discriminate between runs A and B model outputs even in the optimum layer at 40.5 km, keeping in mind that systematic error is ~0.15 ppbv. Nevertheless, we can infer some values of  $\eta$  to be ranging between 0.05 and 0.10, that is consistent with Ricaud et al., (2000) and laboratory data suggesting a value of  $0.05\text{--}0.06\pm0.02$  (Lipson et al., 1997). Note that systematic error can produce a bias in the mixing ratio of the considered species but does not affect the amplitude of its diurnal variation.

Certainly the most interesting results come from the measurements of the diurnal variations of NO<sub>2</sub>, a constituent that has very weak lines within the frequency range of the Bure radiometer. Figure 16 shows the measured and modelled diurnal variations of NO<sub>2</sub> together with the evolution of the a priori (flat line) at 40 km. The measurements are

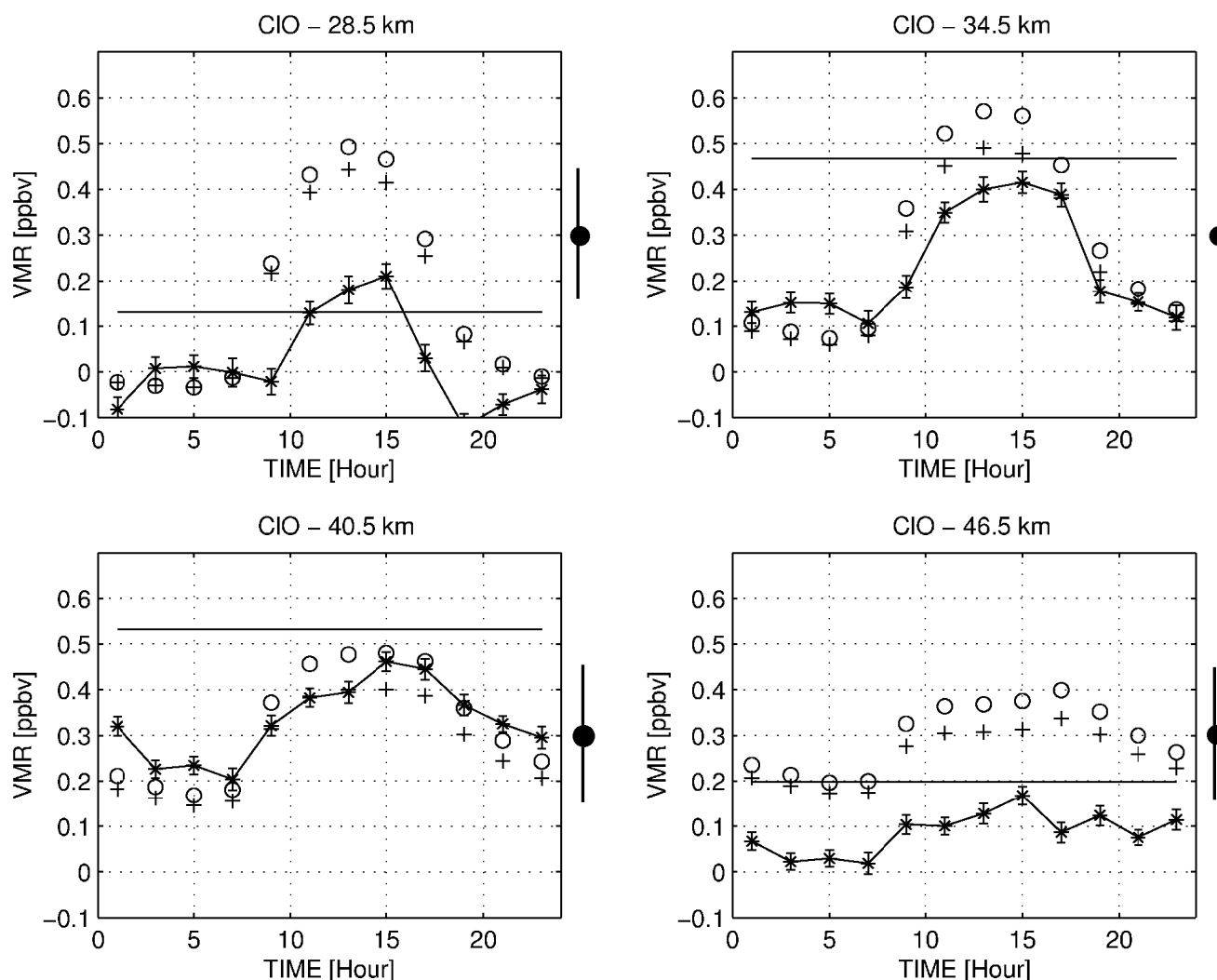


**Fig. 15.** Measured diurnal variations of ClO (stars) at 28.5, 34.5, 40.5 and 46.5 km, together with the a priori value (solid line), and calculations from the 0-D model: run A (crosses) and run B (open circles). Only uncorrelated 1- $\sigma$  error due to the thermal noise is considered in the errorbar. A systematic 1- $\sigma$  error for the Bure measurements (filled circle and thick line) is represented on the right-hand side of each box.

representative of a 3-month average of the retrievals from January to March 1995 into 12 boxes of a 2-hour width from 0 to 24 h.

The orbit of the UARS satellite precesses by a few minutes per orbit, so the local times of the measurements at a given latitude vary by up to 20 min over a 24-hour period, i.e. 24 h over a month by combining ascending and descending nodes. It is then possible to study diurnal variations of constituents like  $O_3$  (Ricaud et al., 1996), ClO (Ricaud et al., 2000), and presently  $NO_2$ . UARS/CLAES  $NO_2$  data have been zonally-averaged within the latitude band  $40^\circ N$ – $50^\circ N$  for the month of February of the years 1992 and 1993 into 12 boxes of a 2-hour width. Both model outputs and satellite data vertical resolutions have been degraded onto the ground-based instrument vertical resolution.

The night-to-day decrease in  $NO_2$  is well detected by the Bure instrument but the amplitude of the diurnal variation is more intense in satellite and model data (6–7 ppbv) than in the Bure data (3–4 ppbv). This underestimation of the amplitude of the diurnal variation, in fact of the nighttime values, is due to the use of an a priori information constant over the 24 hours, since the instrument sensitivity is far from being optimum, namely 0.5, thus the a priori contamination is strong. Nevertheless, the global agreement between measured and modelled variations shows the great potential of the simultaneous analysis of spectra to retrieve both baseline ripples, and different atmospheric constituents, whose emission line (even weak) can be analysed when they are time averaged in order to increase the signal-to-noise ratio, keeping in mind the time frame considered: 3 months.

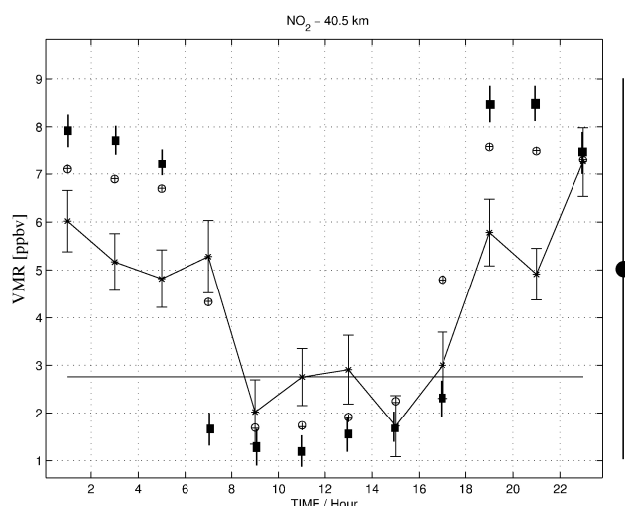


**Fig. 16.** Diurnal variations of  $\text{NO}_2$  at 40.5 km as measured by the ground-based microwave radiometer (stars) and by the UARS/CLAES instrument (filled squares). Ground-based  $\text{NO}_2$  measurements are representative of a 3-month average of the retrievals from January to March 1995. Satellite data have been zonally-averaged within the latitude band  $40^\circ\text{N}$ – $50^\circ\text{N}$  for the months of February 1992 and 1993 in 12 boxes of a 2-hour width. A priori VMR (solid line), and calculations from the 0-D model on 15 January: run A (crosses) and run B (open circles). Note that vertical resolution of the model and of the satellite data has been degraded to match the resolution of the ground-based measurements. Only an uncorrelated  $1\text{-}\sigma$  error due to the thermal noise is considered in the errorbar. A systematic  $1\text{-}\sigma$  error for the Bure measurements (filled circle and thick line) is represented on the right-hand side of the box.

## 5 Conclusions

The present paper has assessed the quality of the measurements made by the microwave radiometer dedicated to the detection of ClO lines around 278 GHz and installed at the Plateau de Bure from 1993 to 1996. This instrument belongs to the international Network for the Detection of Stratospheric Change (NDSC) and is intended to detect changes in the chlorine monoxide temporal evolution at mid-latitude. A new methodology for estimating simultaneously vertical profiles and baseline parameters has been implemented, similar in its philosophy to the method used to analyze microwave measurements from the Odin satellite. Indeed, in addition to ClO, which can be detected from 30–50 km,  $\text{O}_3$  can be retrieved in the altitude range 30–60 km and monthly-averaged  $\text{NO}_2$  can be detected around 40 km.

We can conclude that simultaneous retrievals of  $\text{O}_3$ , ClO, and  $\text{NO}_2$  are qualitatively consistent with model results (photochemical and SLIMCAT models) and independent comparison data (ground-based microwave instrument located at Bern University and UARS satellite instruments), with some differences in the lowermost layers where the incidence of baseline remnants is strong. However, the poor sensitivity of the present instrument, the site location, the baseline per-

turbations, and the slow frequency drift of some components have made it impossible to monitor stratospheric ClO in a quantitative way.

Some improvements are possible. The use of a state-of-the-art detector can reduce the integration time needed for good quality retrieval. A wideband spectrometer can better characterize baseline undulations. Another more elevated site in Europe will certainly help to increase the number of days of good opacity, in order to actually characterize the temporal evolution of ClO at mid-latitude. The present instrument has now returned to the USA in order to be updated.

**Acknowledgements.** The authors would like to thank the teams of the NILU and NCEP databases for their kind contributions in providing us  $\text{O}_3$  data from the NDSC microwave instrument located at the Bern University (Switzerland), and M. Chipperfield (Univ. Leeds, England) for getting output from the chemical transport SLIMCAT model. This project has been funded in France by the Ministry of National Education and Research, CNRS/INSU, and CNES. We would like to dedicate the manuscript to colleagues who accidentally died at the Plateau de Bure in 1999. We finally would like to thank the two anonymous reviewers for their very helpful remarks.

The Editor in chief thanks two referees for their help in evaluating this paper.

## References

- Barath, F. T., Chavez, M. C., and Cofield, R. E., et al.: The upper atmosphere research satellite microwave limb sounder instrument, *J. Geophys. Res.*, 98, 10 751–10 762, 1993.
- Baron, Ph., Ricaud, Ph., de La Noë, J., Eriksson, J. E. P., Merino, F., Ridal, M., and Murtagh, D.: Studies for the Odin Sub-Millimeter Radiometer: II. Retrieval methodology, *Can. J. Phys.*, 80, 341–356, 2002.
- Chipperfield, M. P.: Multiannual simulations with a three-dimensional chemical transport model, *J. Geophys. Res.*, 104, 1781–1805, 1999.
- de La Noë, J., Lezeaux, O., Guillemin, G., Lauqué, R., Baron, P., and Ricaud, P.: A ground-based microwave radiometer dedicated to stratospheric ozone monitoring, *J. Geophys. Res.*, 103, 22 147–22 161, 1998.
- de Zafra, R. L., Jamarillo, M., Barrett, J., Emmons, L. K., Solomon, P. M., and Parrish, A.: New observations of large concentrations of ClO in the springtime lower stratosphere over Antarctica and its implications for ozone-depleting chemistry, *Geophys. Res. Lett.*, 94, 11 423–11 428, 1989.
- Froidevaux, L., Waters, J. W., Read, W. G., Connell, P. S., Kinnison, D. E., and Russell III, J. M.: Variations in the free chlorine content of the stratosphere (1991–1997): Anthropogenic, volcanic, and methane influences, *J. Geophys. Res.*, 105, 4471–4481, 2000.
- Klein, U., Lindner, K., Wohltmann, I., and Künzi, K.: Winter and spring observations of stratospheric chlorine monoxide from Ny-Alesund, Spitzbergen, in 1997/98 and 1998/1999, *Geophys. Res. Lett.*, 27, 4093–4096, 2000.
- Kuntz, M., Hochschild, G., and Krupa, R.: Retrieval of ozone mixing ratio profiles from ground-based millimeter wave measurements disturbed by standing waves, *J. Geophys. Res.*, 102, 21 965, 1997.

- Kuntz, M., Kopp, G., Berg, H., Hochschild, G., and Krupa, R.: Joint retrieval of atmospheric constituent profiles from ground-based millimeterwave measurements: ClO, HNO<sub>3</sub>, N<sub>2</sub>O, and O<sub>3</sub>, *J. Geophys. Res.*, 104, 13 981–13 992, 1999.
- Lary, D. J., Chipperfield, M. P., and Toumi, R.: The potential impact of the reaction OH + ClO → HCl + O<sub>2</sub> on polar ozone photochemistry, *J. Atmos. Chem.*, 21, 61–79, 1995.
- Lezeaux, O.: Mesures micro-ondes d’ozone strato-mésosphérique à partir du sol : Restitution de profils verticaux, validation et interprétation géophysique des résultats, Thèse de l’Université de Bordeaux 1, 1999.
- Lipson, J. B., Elrod, M. J., Beiderhase, T. W., Molina, L. T., and Molina, M. J.: Temperature dependence of the rate constant and branching ratio for the OH + ClO reaction, *J. Chem. Soc. Faraday Trans.*, 93, 2665–2673, 1997.
- Maier, D., Kämpfer, N., and de La Noë, J., et al.: European minor constituent radiometer: A new millimeter wave receiver for atmospheric research, *Int. Journ. of Infra. and Millim. Waves*, 22, 1555–1575, 2001.
- Murtagh, D., Frisk, U., and Merino, F., et al.: An overview of the Odin atmospheric mission, *Can. J. Phys.*, 80, 309–319, 2002.
- Parrish, A., de Zafra, R. L., Solomon, P. M., and Barrett, J. W.: Ground-based technique for millimeter wave spectroscopic observations of stratospheric trace constituents, *Radio Science*, 23, 106–118, 1988.
- Peter, R. and Kämpfer, N.: Short-term variations of mid-latitude ozone profiles during the winter 1994/95, *Proc. Third Europ. Symp. on Polar O<sub>3</sub> Res., Air Pollution Res. Rep. of the EC No 56*, Schliersee, 1995.
- Raffalski, U., Klein, U., Franke, B., Langer, J., Sinnhuber, B.-M., Trentmann, J., Künzi, K. F., and Schrems, O.: Ground-based millimeter-wave observations of arctic chlorine activation during winter and spring 1996/97, *Geophys. Res. Lett.*, 25, 3331–3334, 1998.
- Ricaud, Ph., Brasseur, G., Brillet, J., de La Noë, J., Parisot, J.-P., and Pirre, M.: Theoretical validation of ground-based microwave ozone observations, *Ann. Geophysicae*, 12, 664–673, 1994.
- Ricaud, Ph., de La Noë, J., Connor, B. J., Froidevaux, L., Waters, J. W., Harwood, R. S., MacKenzie, I. A., and Peckham, G. E.: Diurnal variability of mesospheric ozone as measured by the UARS microwave limb sounder instrument: theoretical and ground-based validations, *J. Geophys. Res.*, 101, 10 077–10 089, 1996.
- Ricaud, Ph., de La Noë, J., Lauqué, R., and Parrish, A.: Analysis of stratospheric chlorine monoxide measurements recorded by a ground-based radiometer located at the Plateau de Bure, France, *J. Geophys. Res.*, 102, 1423–1439, 1997.
- Ricaud, Ph., de La Noë, J., Barrett, J., Solomon P., and Parrish, A.: Intercomparisons of ground-based ClO radiometers: Preliminary results in proceedings of the fourth european symposium, *Air Pollution Research Report 66*, Polar stratospheric ozone 1997, 724–727, 1998.
- Ricaud, Ph., Chipperfield, M. P., Waters, J. W., Russell, J. M., and Roche, A. E.: Temporal evolution of chlorine monoxide in the middle stratosphere, *J. Geophys. Res.*, 105, 4459–4469, 2000.
- Roche, A. E., Kumer, J. B., Mergenthaler, J. L., Ely, G. A., Uplinger, W. G., Potter, J. F., James, T. C., and Sterrit, L. W.: The cryogenic limb array etalon spectrometer (CLAES) on UARS: Experiment description and performance, *J. Geophys. Res.*, 98, 10 763–10 775, 1993.
- Rodgers, C. D.: Characterization and error analysis of profiles retrieved from remote sounding measurements, *J. Geophys. Res.*, 95, 5587–5595, 1990.
- Ruhnke, R., Kouker, W., Reddmann, T., Berg, H., Hochschild, G., Kopp, G., Krupa, R., and Kuntz, M.: The vertical distribution of ClO at Ny-Alesund during March 1997, *Geophys. Res. Lett.*, 26, 839–842, 1999.
- Santee, M. L., Manney, G. L., Livesey, N. J., and Waters, J. W.: UARS microwave limb sounder observations of denitrification and ozone loss in the 2000 arctic late winter, *Geophys. Res. Lett.*, 27, 3213–3216, 2000.
- Schneider, N., Lezeaux, O., de La Noë, J., Urban, J., and Ricaud, P.: Validation of ground-based observations of strato-mesospheric ozone, *J. Geophys. Res.*, 108, 4540, doi:10.1029/2002JD002925, 2003.
- Solomon, P. M., de Zafra, R. L., Parrish, A., and Barrett, J. W.: Diurnal variation of stratospheric chlorine monoxide: a critical test of chlorine chemistry in the ozone layer, *Science*, 224, 1210–1214, 1984.
- Solomon, P. M., Connor, B., Barrett, J., Mooney, T., Lee, A., and Parrish, A.: Measurements of stratospheric ClO over Antarctica in 1996–2000 and implications for ClO dimer chemistry, *Geophys. Res. Lett.*, 29, 15, doi:10.1029/2002GL015232, 2002.
- Waters, J. W., Read, W. G., and Froidevaux, L., et al.: Validation of UARS microwave limb sounder ClO measurements, *J. Geophys. Res.*, 95, 10 091–10 127, 1996.
- World Meteorological Organization (WMO): Scientific assessment of ozone depletion: 1994, Rep. 37, Geneva, Switzerland, 1995.
- Zommerfelds, W. C., Künzi, K. F., Summers, M. E., Bevilacqua, R. M., Strobel, F., Allen, M., and Sawchuck, W. J.: Diurnal variations of mesospheric ozone obtained by ground-based microwave radiometry, *J. Geophys. Res.*, 94, 12 819–12 832, 1989.